

# Improving of the fatigue lifetime prediction of screw for a large range of mean stresses

A. Duval, P. Robinet, F. Trivaudey and P. Delobelle  
 Laboratoire de Mécanique Appliquée R. Chaléat, UMR C.N.R.S. 6604  
 Université de Franche-Comté, 24 Chemin de l'épitahe, 25000 Besançon, FRANCE

## **Abstract:**

From a Finite Element analysis, the stress distribution in the notch of axisymmetric and highly loaded notched samples has been calculated. The samples are shaped like a thread root. We propose a simplified method of sizing screws for a large range of mean stresses. So, a local Haigh's diagram (at the thread root) is built from experimental the Haigh's diagram derived from smooth or notched samples.

## **I – Introduction**

When trying to predict the fatigue lifetime of a screw used in a highly loaded assembly, the designer has to handle two types of difficulties. The first one is to include the effects of the mean stress on the damage. The second one, related to the geometry of the screw, is to know the influence of the notch effect on the damage in the thread root. The Haigh's and Goodman's diagram help us to solve the first problem when the mechanical properties of the material are known. Indeed, they give the endurance domain in which the applied and the mean stresses have to be located. The second difficulty is partly overcome thanks to Neuber's method or the method of the gradient since they take into account the effect of stress concentration inside the thread root.

Here, the method is based on an elasto-viscoplastic analysis leading to the knowledge of the local stress and strain components. Then, a multiaxial failure criterion derived from the damage rules is locally applied. This leads to a simple method of building the Haigh's local diagram. The global method follows four steps:

- i) Determination for the considered steel of the elastoplastic behaviour rules under uniaxial loading with or without mean stress.
- ii) Determination of the damage rules leading to the rupture criteria as well as to the cumulative calculations.
- iii) Theoretical and experimental studies of notched axisymmetric samples shaped like a thread root.
- iv) Study of the fully screw-bolt assemblage.

We will present here the first three steps.

## **II – Materials and experimental methods**

The screw steel studied here is a 38CD4 steel oil quenched from 850°C then stress relieved at 600°C for one hour. This results in a fully martensitic microstructure. Its weight composition is as follows:

C %	Mn %	Si %	S %	P %	Cr %	Mg %	Fe %
0.36	0.792	0.232	0.028	0.016	1.039	0.175	balance

$$K_t = \left[ 1 + \frac{1}{\sqrt{\left(\frac{1}{1.197K_p}\right)^2 + \left(\frac{1}{1.871K_q}\right)^2}} \right]^{\sqrt{\cos(a/2)}} \quad \text{with} \quad \begin{cases} K_p = \sqrt{\frac{t}{r} \frac{d/D}{1-d/D}} + 1 - 1 \\ K_q = \frac{1}{\sqrt{r/t}} \\ t = \frac{D-d}{2} \end{cases} \quad [1]$$

The whole set of tests were performed at room temperature, on smooth samples as well as on axisymmetric notched samples shaped like a thread root of a screw with a null pitch.

The dimensions of the notched samples with triangular profile (external diameter  $D = 6\text{mm}$ , diameter at the notch root  $d = 4.78\text{mm}$ , angle between the sides of the notch  $\alpha = 60^\circ$  and  $\alpha = 120^\circ$  and junction radius of the two sides at the notch root  $r = 0.35\text{mm}$  and  $r = 0.29\text{mm}$ ) leads, following equations [1], to the geometric stress concentration factor  $K_t$  equal respectively to 2.41 and 2.1. Some specimens with circular notch leading to  $K_t = 1.5$  were also tested.

For these samples, the applied and mean stresses  $\Delta s_E / 2$ ,  $s_{moyE}$  are calculated from the normal section at the site of the notch.

### III – Results and Analysis

#### 3.1) Main mechanical properties of the steel

This steel has the following characteristics :

A high yield stress  $R_{0.2\%}$  around 1000 MPa and a failure stress  $R_m$  close to 1100 MPa together with a fairly good ductility at failure ( $>10\%$ ). Note that there is quite an important dispersion on these two values between the different sets of samples because of the low reproductibility of the heat treatment.

As far as the cyclic properties between symmetric imposed strains are concerned, a continuous softening is observed up to the failure. A plateau for the first quarter of cycle is visible together with the well curved form of the cycles related to an important Bauschinger effect. The cyclic curves measured at a quarter of cycle, at one cycle, at half failure number of cycles  $N_R/2$  and at the failure number of cycles  $N_R$  are drawn in Figure 1. When the cyclic loading is no longer symmetric, an important progressive strain can be shown, when the maximal stress  $s_{Max}$  is fixed at 990 MPa and when the mean stress  $s_{moy}$  is less than 280 MPa (Fig. 2). The strong dispersion between the two sets of samples, due to the heat treatment, can also be noted.

At room temperature, the viscosity of this steel is too small to be considered. Indeed, after 48 hours, the relaxed amplitude related to the initial stress amplitude is always less than 10%.

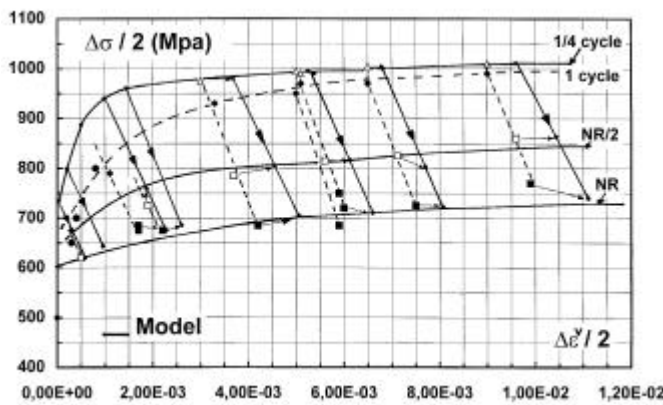


Fig.1: Monotonic (1/4) and cyclic curves  
 $\Delta s / 2 = f(\Delta e^v / 2)$  at one,  $N_R/2$  and  $N_R$  cycles.  
 Experiments and modelling

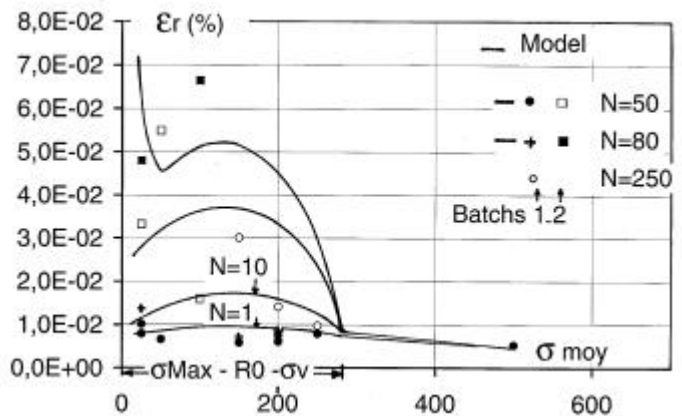


Fig.2 : Ratchet strain as a function of  $s_{moy}$  for different  $N$ .  
 Experiments and modelling

#### 3.2) Formulation of the constitutive laws

According to the previous experimental observations, a unified viscoplastic formulation with a yield threshold, two kinematic hardening ( $a_j^{(1,2)}$ ) and one isotropic hardening ( $Y$ ) variables has been chosen. The general rules are :

$$\begin{aligned}
e_{ij}^T &= e_{ij}^e + e_{ij}^v & \text{with } \dot{e}_{ij}^e &= \frac{1+u}{E} \dot{s}_{ij} - d_{ij} \frac{u}{E} \dot{s}_{kk} \\
\text{and } \dot{e}_{ij}^v &= \frac{3}{2} \dot{e}_0 \left\langle \frac{J_2(s - a) - Y^{st}}{N} \right\rangle^n \frac{\dot{s}_{ij} - a_{ij}}{J_2(s - a)} & \text{where } \bar{e}^v &= \frac{2}{3} \dot{e}_{ij}^v \dot{e}_{ij}^v \frac{1}{2} \\
a_{ij} &= a_{ij}^{(1)} + a_{ij}^{(2)} & & [2] \\
\dot{a}_{ij}^{(1)} &= p_1 \frac{2}{3} Y_1 \dot{e}_{ij}^v - a_{ij}^{(1)} \bar{e}^v \frac{\dot{\sigma}}{\sigma} & \text{with } a_{ij}^{(1)}(0) &= 0 \\
\dot{a}_{ij}^{(2)} &= p_2 \frac{2}{3} Y_2 \dot{e}_{ij}^v - a_{ij}^{(2)} \bar{e}^v \frac{\dot{\sigma}}{\sigma} & \text{with } a_{ij}^{(2)}(0) &= 0 \\
Y^{st} &= R_0 + Y \quad \text{and} \quad \dot{Y} = b (Y^\# - Y) \bar{e}^v & \text{with } Y(0) &= 0 \quad \text{and} \quad Y^\# < 0
\end{aligned}$$

In these equations :  $J_2(s - a) = \frac{3}{2} (s_{ij} - a_{ij})(s_{ij} - a_{ij}) \frac{\dot{\sigma}}{\sigma} = s_v + Y^{st}$  where  $s_{ij}$  and  $a_{ij}$  (or  $a_{ij}$ ) are the deviators tensor components,  $d_{ij}$  the Kronecker symbol,  $\langle \rangle$  the Macauley brackets, that is  $\langle x \rangle = xH(x)$ , where  $H(x)$  is the Heaviside function.

The integration of the rules up to  $N_R$  (number of cycles to failure), with the identified model leads to the responses given in Figures 1 and 2. However, it is possible to choose a set of parameters, for a given number of cycles, that is, using new values for the parameters  $Y^{st}$  and  $p_1$ . Thus, at the  $1/4$  of cycle,  $Y^{st}$  is equal to  $R_0$  and at the stabilized cycle,  $Y^{st}$  is equal to  $(R_0 - |Y^\#|)$ , at least for the greatest strain amplitudes. We can thus obtain directly the shape and the amplitude of the cycles at  $1/4$  of cycle, for the cycle at  $N_R/2$  and  $N_R$ , integrating the rules on only one cycle (Fig.1). For this steel with high yield stress, the progressive strain is on one hand due to the non-linearity of the kinematic variables ( $p_1$  and  $p_2$ ) and on the other hand to the cyclic softening. We can see in Figure 2, that the amplitude of the ratchet zone is fairly well modelled (ratchet zone  $\approx s_{Max} - R_0 - s_v$ ) but although that the ratchet is compatible with experimental results even if its amplitude is over-estimated.

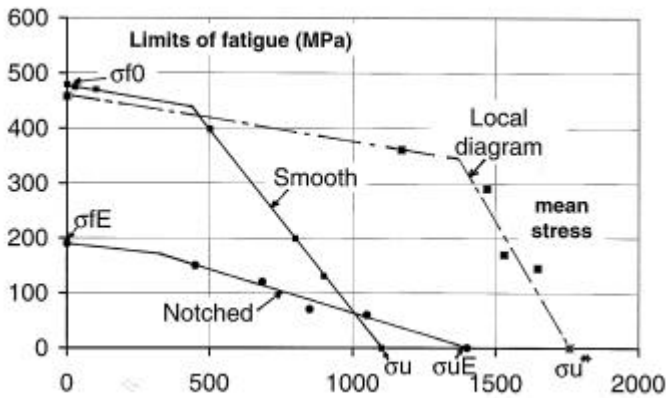


Fig.3 : Different Haigh's diagrams for smooth and notched samples. Determination of the local diagram.

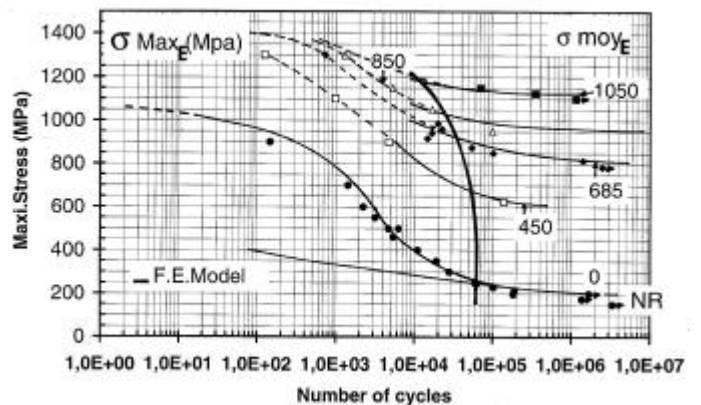


Fig.4 : Woehler's curves of notched specimens for different mean stresses. Experiments and F.E. calculations.

### 3.3 Fatigue properties and modelling

From the Woehler curves the Haigh's diagram can be built for smooth samples, giving the evolution of the endurance stress related to the mean stress  $s_f = f(s_{moy})$  (Fig.3). From an uncoupled local approach, the damage variable  $D$  is taken with a formulation of the ONERA type  $\{1\}\{2\}$ :

$$dD = D^a \bar{p} \cdot P_M \cdot J_{2Max} s_u^* \cdot s_{f0} \left( J_2 \frac{\sigma^D s}{\epsilon} \frac{\dot{\sigma}}{2} / M(\bar{p}) \frac{\dot{\sigma}}{\epsilon} \right)^b dN \quad [3]$$

Taking into account the non-linearity of the Haigh's diagram and the effect of the triaxiality on the ultimate stress  $s_u$ , the integration of equation [3] gives the number of cycles to failure  $N_R$ .

$$N_R = \frac{1}{aM_0^{-b}} \frac{\langle s_u^* - J_{2Max}(s) \rangle}{\langle J_2 \frac{\sigma^D s}{\epsilon} \frac{\dot{\sigma}}{2} - s_{f0} f(\bar{p}) \rangle} \left\langle \frac{J_2 \frac{\sigma^D s}{\epsilon} \frac{\dot{\sigma}}{2}}{f(\bar{p})} \right\rangle^{-b} \quad \text{with :}$$

$$\bar{p} = \frac{s_{ii}}{3}, \quad p_M = \text{Max}(0, \bar{p}), \quad \bar{p} = (1 - l) \bar{p} + l p_M - \frac{1}{3} J_2 \frac{\sigma^D s}{\epsilon} \frac{\dot{\sigma}}{2},$$

$$J_2 \frac{\sigma^D s}{\epsilon} \frac{\dot{\sigma}}{2} = \frac{1}{2} \sqrt{\frac{3}{2} (s_{ijMax} - s_{ijmin})(s_{ijMax} + s_{ijmin})}, \quad J_{2Max}(s) = \text{Max}(0, J_2(s)), \quad [4]$$

$$J_2(s) = \sqrt{\frac{3}{2} s_{ij} s_{ij}}, \quad f(X) = (1 - 3bX)Q + b'(s_u^* - 3X)(1 - Q) \quad \text{where}$$

$$Q = H \frac{b' s_u^* - 1}{b' - b} - 3X \frac{\dot{\sigma}}{\epsilon} \quad \text{with } X = \bar{p} \text{ or } \bar{p} \quad \text{and} \quad s_u^* = s_u \exp \left( \frac{3\bar{p} + J_{2Max} \frac{\sigma^D s}{\epsilon} \frac{\dot{\sigma}}{2}}{J_{2Max}(s)} - 1 \right).$$

In equations [3] and [4], during each cycle,  $\bar{p}$  and  $\bar{p}$  are the hydrostatic mean stress and the hydrostatic maximum stress,  $J_{2Max}(s)$  the maximal equivalent von Mises stress,  $s_u$  the ultimate stress in a uniaxial tensile test and  $s_{f0}$  the endurance stress at null mean stress. Note that  $s_u^* = s_u$  for uniaxial tests on smooth specimens and for symmetric cyclic tests ( $\bar{p} = 0$ ) on notched samples. For  $\bar{p} \neq 0$  on notched samples,  $s_u^* > s_u$ .

The whole experimental database let us identify all the coefficients involved in the relations [4], that is:

- tensile tests without mean stress,  $\frac{1}{aM_0^b}, b, s_u, s_{f0}$ ,
- tensile tests with mean stress,  $b$  and  $b'$ ,
- torsion tests,  $l$ .

During the correlation analysis ( $N_R \text{ calculated} = f(N_R \text{ experimental})$ ), the experimental dispersion due to the heat treatment has been taken into account. Its single effect is to modify the experimental value of  $s_u$ . This leads to a fairly good correlation (factor 2) although the experimental dispersion on the database is important.

#### **IV – Study of notched axisymmetric samples**

Figure 4 shows the Woehler curves of notched samples, which lead to the Haigh's diagram for this geometry,  $s_{fE} = f(s_{moyE})$  (Fig.3). For  $s_{moyE} = 0$ , we obtain something like  $s_{f0}/s_{f0E} = 2,46 \gg K_t$ . However, the uniaxial tensile tests up to the failure give  $s_{uE} \gg 1400 \text{ MPa}$ , which corresponds to the linear extrapolation of the experimental points with mean stress (Fig.3).

According to the different experimental applied loadings and using the rules [2], a lot of monotonic or cyclic F.E. calculations have been performed (integration over some hundreds of cycles). The calculated responses are then compared to the experimental results. The agreement is generally correct as shown in Figure 5 for a monotonic test. A study of the parametric sensibility of the results

shows that the isotropic hardening variable, describing the cyclic softening and responsible for the stress redistribution at the notch root, is the first component driving the progressive strain. This result is in opposition with the test on smooth samples. We note a strong geometric effect due to the quite high value of  $K_t$ .

Looking at the stress redistribution, for a symmetric loading, the profile of the von Mises stress  $J_{2L}(\sigma)$  along the ligament is clearly continuously decreasing during the cyclic loading to reach the profile obtained for the stabilized cycle. This one can be quickly calculated by integrating on only one cycle the behaviour rules (Fig.1). These rules are directly identified for the number of cycles to failure  $N_R$  (Fig.1). This results can be checked a posteriori in Figure 6 where the Woehler curves have been obtained by post-processing with the relations [4] and using the laws identified with one cycle, at  $N_R/2$  and  $N_R$  (the elastic solution is also represented). The prevision of the number of cycles to failure is correct considering the rules for the stabilized cycle. Moreover, the good agreement of  $N_R$  on the whole curve related to elastic and plastic cycles shows that when  $s_{f0E} < (R_0 + s_v)/K_t = 249 \text{ MPa}$ , the cycles are elastic {3}.

Looking at the stress distribution for non symmetric loadings, it can be noted that for  $s_{MaxE} < s_{moyE} + (R_0 + s_v)/K_t$  (this limit is drawn Fig.4), the cycles are elastic,  $J_{2L}(Ds/2) = K_t(Ds_E/2)$  at the notch root, and the stress redistribution obtained at the end of the first quarter of cycle is stable during cycling. Thus, the prevision of  $N_R$  has been obtained by post-processing over one elastic cycle with the law identified at  $1/4$  cycle. The results are correct as shown in Figure 4 (right part of the Woehler's curves).

For  $s_{MaxE} > s_{moyE} + (R_0 + s_v)/K_t$ , first the mean stress is fully relaxed at the notch root, and then, the amplitude  $J_{2L}(Ds/2)$  starts to decrease and then increases again before remaining stable. This last period is related to the local ratchet (left part of the Fig. 4). The amplitude of the decrease can be easily estimated from F.E. calculations leading to the factors of stress intensity  $K_p$  as a function of  $Ds_E/2$ , respectively for the laws at the first cycle  $K_p^0$  and at  $N_R$ ,  $K_p^{\infty}$ . The unknown amplitude  $(K_p^0 - K_p^{\infty})Ds_E/2$  can thus be obtained. However, the increase of  $J_{2L}(Ds/2)$  is more difficult to evaluate. The only way to calculate it, is to use abacus built from F.E. calculations and to give the local ratchet rate at the notch root as a function of  $Ds_E/2$  and  $s_{moyE}$ . Thus, the local stress state should be known,  $s_{moyL} @ 0$  and  $J_{2L}(Ds/2)$  estimated with the previous method and then  $N_R$  is deduced from the Woehler's curve on smooth samples at  $s_{moy} = 0$ . For small values of  $N_R$  ( $N_R < 10^3$ ) the previsions are good because the local ratchet rate is fairly well known. The extrapolation of the calculation is done on less than a decade. For higher values of  $N_R$ , ( $N_R @ 10^4$ ) the accuracy is not so good because of the ratchet rate is not precisely known anymore.

The F.E. method, using the law at  $1/4$  of cycle of the evolution for a monotonic test, with the coefficients  $K_m = 3p_{MaxL}/s_{MaxE}$  and  $K_p = J_{2MaxL}(s)/s_{MaxE}$  as a function of  $s_{MaxE}$  (or  $s_{moyE}$ ) let us estimate the local Haigh's diagram (Fig.3). Hence, for a given point of the global diagram of the notched specimens, its ordinate is multiplied by  $K_t$  and its abscissa by  $K_m(s_{MaxE})$ . The local rupture stress for a

monotonic test is given by  $s_u^* = s_u \exp d \frac{\infty}{\infty} \frac{3p_{MaxL}}{J_{2MaxL}(s)} - 1 \frac{\ddot{\circ}}{\ddot{\circ}} = s_u \exp d \frac{\infty}{\infty} \frac{K_m}{K_p} - 1 \frac{\ddot{\circ}}{\ddot{\circ}}$ . Moreover, it could be

shown (from the knowledge of  $s_{f0}, s_{f0E}, s_u$  and  $s_{uE}$ ) that a unique dimensionless Haigh's diagram can be built for smooth and notched specimens {3}. It is thus possible to work with a diagram (smooth) or the other (notched).

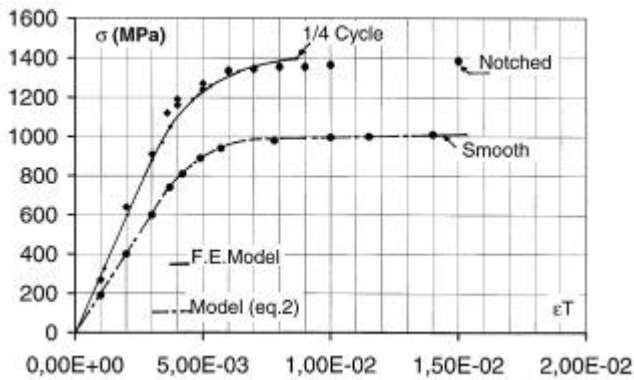


Fig.5 : Monotonic stress-strain curves for smooth and notched specimen. Experiments and modelling.

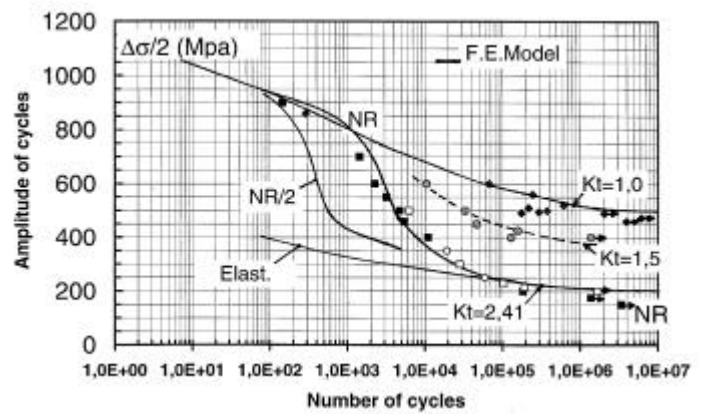


Fig.6 : Woehler's curves for smooth and notched specimens ( $s_{moy} = 0$ ). Experiments and F.E. calculations.

## V – Conclusion

For the studied steel, the stress redistribution at the notch root has been shown to be mainly managed by the isotropic hardening variable describing the cyclic softening. Thus, a simple method is proposed, knowing the parameters  $K_t, K_p, K_m$  (F.E. calculations) and  $s_{f0}, s_{f0E}, s_u$  and  $s_{uE}$  (experimental data), to deduce from the global diagram (smooth or notched specimen) the local Haigh's diagram at the notched root. In this case, the cycles are elastic.

When the cycles are plastic with  $s_{moyE} = 0$ , the integration of the behaviour rules for the stabilized cycle following by the post-processing calculations of the failure rules allow us to estimate  $N_R$ . However, if  $s_{moyE} \neq 0$ , the local mean stress is fully relaxed, the amplitude of the cycle starts to decrease and then increases because of the local ratchet strain. In this case, it is more difficult to estimate precisely  $N_R$  if the local ratchet rate is not precisely known.

## **Acknowledgments :**

This study has been supported by the society FORMER-DELLE-90101.France.Cedex

## **References:**

- {1} - CHABOCHE J.L. Rev. Fr. Mec., n°9, 1974, 50.
- {2} - CHAUDONNERET M. , J. Eng. Mat. Techn., Vol 115, 1993, 373-379
- {3} - DUVAL A., ROBINET P., TRIVAUDEY F., DELOBELLE P., Rapport 7, contrat FORMER/LMARC, 1999